Liquid Crystals
Publication details, including instructions for authors and subscription information:
http://www.informaworld.com/smpp/title~content=t713926090

Momentum space imaging of a liquid crystal filled Fabry-Perot

M. McSweeney[a]; G. W. Bradberry[a]; J. R. Sambles[a]; G. S. Taylor[b]
[a] Thin Film and Interface Group, Department of Physics, University of Exeter, Exeter, England [b] G.E.C. Marconi Ltd., Hirst Research Centre, Hertfordshire, England

To cite this Article McSweeney, M. , Bradberry, G. W. , Sambles, J. R. and Taylor, G. S.(1995) 'Momentum space imaging of a liquid crystal filled Fabry-Perot', Liquid Crystals, 18: 4, 539 — 543
To link to this Article: DOI: 10.1080/02678299508036656
URL: http://dx.doi.org/10.1080/02678299508036656

LIQUID CRYSTALS, 1995, VOL. 18, NO. 4, 539–543

Momentum space imaging of a liquid crystal filled Fabry–Perot

by M. McSWEENEY*, G. W. BRADBERRY, J. R. SAMBLES
and G. S. TAYLOR†

Thin Film and Interface Group, Department of Physics, University of Exeter,
Stocker Road, Exeter EX4 4QL, England
† G.E.C. Marconi Ltd., Hirst Research Centre, Elstree Way, Borehamwood,
Hertfordshire WD6 1RX, England

(*Received 25 April 1994; in final form 7 September 1994; accepted 17 September 1994*)

Liquid crystal layer characteristics have for some time been determined by analysis of the optical guided modes supported within such layers. A novel technique for guided mode analysis, relying on scattering and re-radiation of light from a liquid crystal filled Fabry–Perot, is presented here and compared with a more standard technique, where the transmissivity of light through such a structure, as a function of the angle of incidence, is measured. The new technique which we label 'momentum space imaging' is found to hold some advantages over traditional methods, with data acquisition on the millisecond time-scale and full liquid crystal layer characterization being achievable with minor modification to existing theoretical multilayer modelling.

1. Introduction

There has been much recent interest in the optical characterization of liquid crystals by analysis of the guided modes supported within a thin liquid crystal layer [1–4]. Such guided modes may be excited by varying the angle of incidence of a laser beam upon a liquid crystal layer encapsulated in a silver-mirror Fabry–Perot type structure. At particular incidence angles, the momentum of the incident light along the liquid crystal layer exactly matches the momentum of a resonant mode within that layer. Evanescent coupling of light through one silver layer into the liquid layer occurs, causing a drop in the reflectivity for this particular angle. Modes of various momenta may therefore be excited by varying the incident angle, and so a reflectivity versus angle curve consists of a series of reflectivity minima [1–3]. Liquid crystal layer characteristics are determined by comparison of these angle dependent reflectivities with modelled predictions based on Berreman's 4×4 matrix theory [5].

Problems with this technique are the time scales of minutes involved in making reflectivity versus angle scans, requiring thermal and dynamic sample stability, the possibility of beam spot movement across the sample as it is rotated, and the fact that each scan probes the liquid crystal layer in the plane of incidence of the beam only, giving no information on mode details at azimuthal angles out of the plane of incidence. Multiple scans, using different input light polarizations or cell orientations, are required for complete liquid crystal layer characterization. Cell movement between each scan may also result in a slightly different cell region being probed each time, leading to small inconsistencies in parameter determination.

Presented here is a novel technique for liquid crystal layer characterization, yielding an 'instant' indication of mode momenta at all azimuthal angles. This involves shining radiation normally into the resonant Fabry–Perot and imaging the radiation scattered from inside the cell. This scattered radiation has an angular dependent variation which is characteristic of the liquid crystal director in the cell. Imaging of all the re-radiated pattern, momentum space imaging, thus gives very direct information on the full director profile in the liquid crystal. The re-radiated light is in fact emitted as circular and elliptical cones of radiation, corresponding to the ordinary and extraordinary modes of the system, and is recorded via a C.C.D. camera. This provides a direct map of the two-dimensional momentum space for the mode wave vectors in the plane of the system.

In this study, an approximately $6\,\mu$m thick homogeneously aligned nematic liquid crystal layer (Merck Ltd E7) is confined between glass plates, each coated with a silver mirror. Thin layers of silicon oxide (SiO) were deposited by thermal evaporation on to the silver layers at an evaporation angle of 60°, in order to form an alignment

* Author for correspondence.

0267–8292/95 $10·00

layer which gives flat-in-the-plane homogeneous alignment of the liquid crystal director perpendicular to the plane of SiO evaporation. The cell was assembled with the surface alignment directions parallel, resulting in an untwisted director profile, **n**, through the liquid crystal layer, with the director everywhere parallel to the plane of the bounding plates. The optical response of the layer is essentially that of a uniaxial slab, with boundary conditions dictated by the silicon oxide and silver layers.

2. Experimental

The cell was constructed using two low index ($n = 1{\cdot}457$ at 632·8 nm) glass plates. Thin silver layers (≈ 33 nm) were deposited by vacuum evaporation. This layer thickness is appropriate for good optical coupling into the liquid crystal layer, while still providing good reflective layers for guided mode propagation. The layers were characterized using the surface plasmon polariton resonance excited at the silver/air interface by *p* polarized (transverse magnetic) light incident on the back face of the silver film, using prism coupling and a matching fluid. The form of the reflectivity curve as a function of angle of incidence is dependent upon the silver film thickness and its optical permittivity, so comparison with a theoretical prediction based on Fresnel equations yields values for these parameters.

Results for the silver film were $\epsilon = -17{\cdot}81 (\pm 0{\cdot}03) + 0{\cdot}65i (\pm 0{\cdot}03i)$ and $t = 33{\cdot}2$ nm ($\pm 0{\cdot}5$ nm).

Next, the SiO layers were deposited and characterization of the SiO overlayers was then achieved in a similar manner to that for the silver layers. The SiO overlayer displaces the surface plasmon resonance angle, the displacement being dependent upon the optical thickness of the SiO layer. In fitting Fresnel theory to the SiO data, it is found necessary to lock the value of the layer thickness at some thickness, in this case 20 nm, as determined by the change in frequency of a quartz crystal oscillator situated in the evaporation beam, otherwise there is a degeneracy in the parameter determination.

With the silver and SiO layers characterized, the cell was then assembled using 3·5 μm mylar spacers, with the SiO evaporation directions parallel. It was then filled with E7 liquid crystal by capillary action.

This complete cell was then characterized using a variation of the traditional attenuated total internal reflection technique referred to earlier, for subsequent comparison with data obtained by the scattering method.

The cell was placed on a computer controlled rotating table such that the angle of incidence of a helium–neon ($\lambda = 632{\cdot}8$ nm) laser beam could be varied and the transmitted light intensity recorded. Data sets were taken using both *s* and *p* polarized light, with the director perpendicular to the plane of incidence, thereby probing

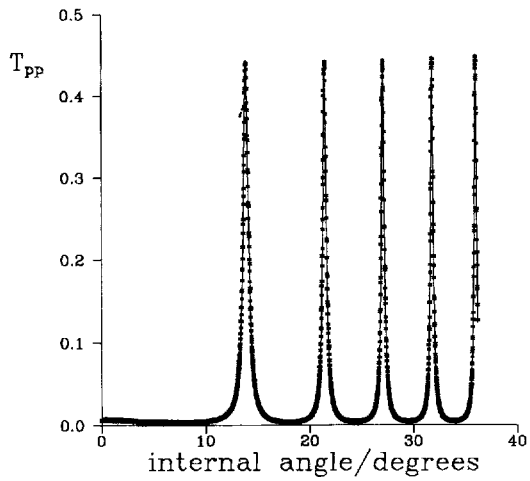

Figure 1. Comparison of theory (full line) to data (crosses) for *p* polarized transmitted light with *p* polarized incident (T_{pp}), with the director normal to the plane of incidence ($\lambda = 632{\cdot}8$ nm).

dielectric permittivity parallel to the director, $\epsilon_\parallel$, for the *s* modes and perpendicular to the director, $\epsilon_\perp$, for the *p* modes. Transmissivity versus angle scans consist of a series of transmissivity maxima—each maximum occurring when the mode coupling condition is satisfied. Data sets were matched with theory generated by a general anisotropic multilayer modelling program [5]. Fixed values of $\epsilon_\perp$ and $\epsilon_\parallel$ for the liquid crystal layer were used in fitting theory to the various data sets, with only a small variation in liquid crystal layer thickness being allowed between data sets. This was to be expected, since the glass plates forming the cell cannot be assembled precisely parallel, inevitably resulting in a small thickness variation (< 10 nm) across the liquid crystal layer. When performing multiple scans, slight movement of the equipment between each scan results in a different cell region, and therefore thickness, being probed each time.

A sample fit of a theoretical transmissivity curve to a data set is shown in figure 1. Liquid crystal layer parameters were found to be $\epsilon_\perp = 2{\cdot}300 (\pm 0{\cdot}001) + 3 (\pm 1) \times 10^{-4}i$, $\epsilon_\parallel = 3{\cdot}002 (\pm 0{\cdot}001) + 6 (\pm 1) \times 10^{-4}i$ and $t = 5{\cdot}69$ μm ($\pm 0{\cdot}02$ μm).

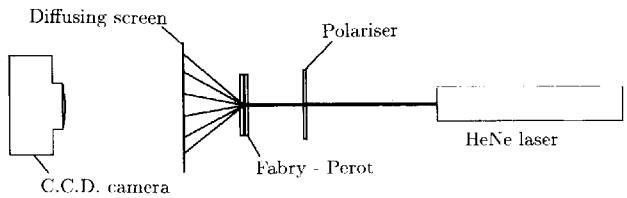

Figure 2. Schematic representation of the experimental arrangement used to obtain the momentum space imaging data presented in this work.

3. Momentum space imaging

In the new type of experiment, following the preceding characterization, helium–neon laser light was made normally incident upon the Fabry–Perot as shown in figure 2. The mechanism whereby the incident radiation is scattered into guided modes supported in the liquid crystal layer is not clearly understood, however the process is likely to occur in the SiO or within the liquid crystal layer itself, as a result of director fluctuations. Strong scattering into modes did not occur for light incident at all points on the cell, but only at regions where the liquid crystal layer thickness was appropriate for the excitation of a Fabry–Perot mode. Contours of constant thickness were observed as continuous re-radiation lines in the cell under laser illumination, providing a thickness 'map' of the cell. Two sets of these 'contour lines' could be excited, depending on the incident light polarization; light polarized perpendicular to **n** sensed $\epsilon_\perp$, whereas light polarized parallel to **n** sensed $\epsilon_\parallel$. The optical thickness of the cell therefore differs for each polarization and so 'contour lines' appear in different positions for each input polarization. Scattered, transmitted, light intensity patterns were allowed to fall on to a diffusing screen, the pattern formed then being focused on to a C.C.D. camera array.

4. Data analysis

A typical C.C.D. image of the scattered pattern for incident polarization *OY* is shown in figure 3(*a*). The intense, unscattered central laser spot was masked on the screen and so is not apparent. Knowing the image magnification factor and with accurate measurement of the

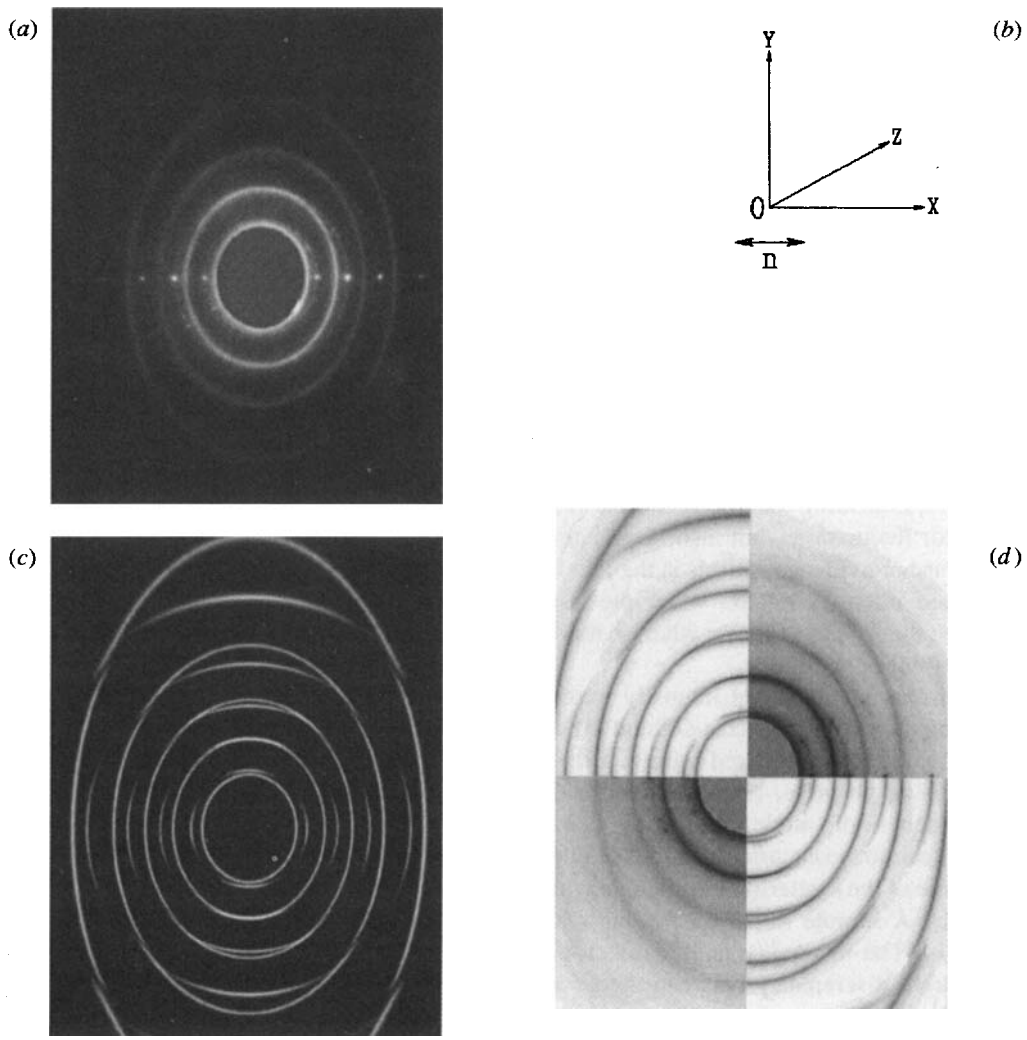

Figure 3. (*a*) The C.C.D. momentum space image used for analysis, with incident polarization in the plane *OYZ* and the director along *OX*. (*b*) The axis convention used in the text. (*c*) A theoretically generated image for comparison with (*a*). (*d*) superposition of reverse contrast experimental and theoretical images; the upper right and lower left quadrants are experimental.

distance from the cell to the screen, mode excitation angles are readily determined, to an accuracy of $\pm 0{\cdot}1°$.

Two sets of modes are apparent: circular 'ordinary' and elliptical 'extraordinary' modes. Upon investigation of these output modes, it is observed that the ordinary modes have polarization lying in the *OYZ* plane, using the axes defined in figure 3 (*b*), since light of this polarization remains perpendicular to the director and therefore senses only $\epsilon_\perp$, irrespective of propagation direction through the liquid crystal layer. This symmetry results in the generation of circular rings of scattered modes. Elliptical lines of scattered modes are of polarization lying in the plane *OZX*. The permittivity sampled by this polarization is directionally dependent, ranging from purely $\epsilon_\parallel$ for light propagating in the *YZ* plane, and polarized in the *OX* direction, to a combination of $\epsilon_\perp$ and $\epsilon_\parallel$ for propagation in the *XZ* plane, with polarization in the plane *OZX*. So it is seen that for light plane polarized parallel to the *OY* axis, incident on the cell, two orthogonal polarization sets, polarized in the *OYZ* and the *OZX* planes, are re-radiated. Polarization conversion therefore must occur either upon scattering or multiple reflection within the cell. As can be seen in figure 3 (*a*), scattering into the circular ordinary modes is weaker than for the extraordinary modes, even though the ordinary modes are excited by the incident light polarization *OY*. This depolarized scattering is consistent with scattering via thermal fluctuations in the nematic director [6]. An intensity versus angle plot showing the extraordinary mode intensities along the *OY* axis of figure 3 (*a*) is shown in figure 4 (*a*). This is compared with a theoretical plot of intensity variation due solely to scattering via director fluctuations [7], using the liquid crystal layer parameters gained from the transmissivity versus angle scans. The form of the data and experimental curves clearly differs, indicating that the scattering is not solely due to director fluctuations, but also occurs at the alignment layers. Further evidence for this is the fact that scattering of reduced intensity occurs when the liquid crystal is heated into the isotropic phase, when scattering within the liquid crystal is negligible.

The angular positions of the mode intensity maxima were measured along the two image axes *OX* and *OY* and these mode excitation angles compared with theoretical transmissivity versus angle plots, calculated neglecting the angular dependence of mode intensities due to scattering, since this cannot be accurately modelled due to our lack of knowledge of the scattering mechanism within the alignment layers. A sample fit for data along *OX* is shown in figure 4 (*b*). The resonance angles match very well, but there is slight discrepancy between theory and data, with angular displacements of $\approx 0{\cdot}1°$ between data and theoretical mode intensity maxima. These angular displacements are of the order of the experimental error for the determination of the mode excitation angles; however errors incurred in angle determination are primarily systematic, and so shifts of theoretical modes relative to experimental modes would be expected to be in the same direction. In figure 4 (*b*), theoretical mode positions are displaced to either side of the experimental, indicating that

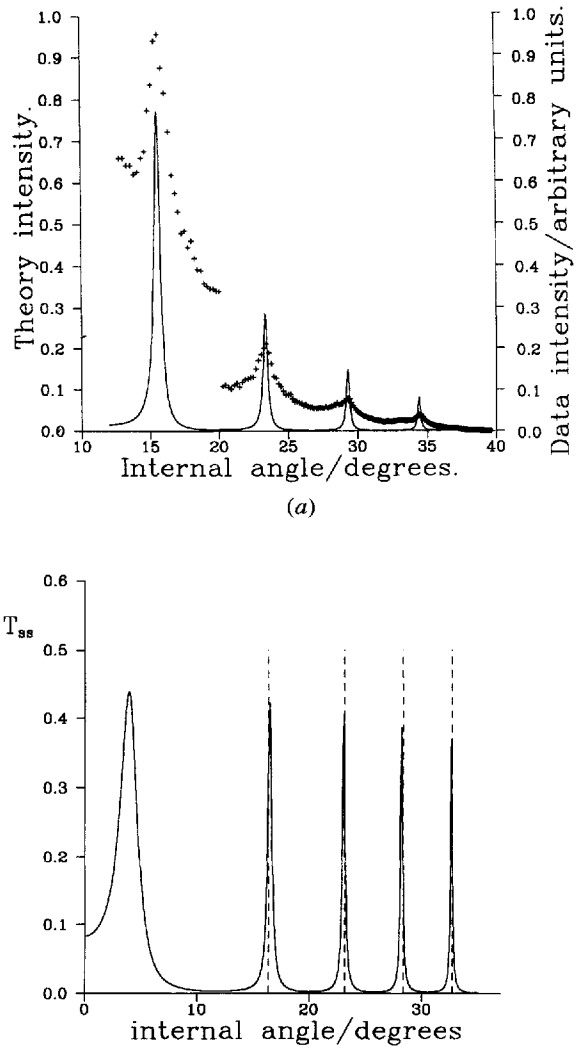

Figure 4. (*a*) Comparison of intensity versus scattering angle along the *OY* axis of figure 3 (*a*) (crosses) with the theoretical model based solely on depolarized scattering via director fluctuations (solid line). Input polarization is in the plane *OYZ* and the output is along *OX*. The break in the data at $\approx 20°$ is due to a scaling of the lower angle data relative to the higher angle data to compensate for attenuation of the central region of the image, figure 3 (*a*), by a filter during data acquisition. The discontinuity in the resulting data plot is present due to scattering at the edge of the attenuator. (*b*) Comparison of mode excitation angles calculated from the *OX* axis of the C.C.D. image, figure 3 (*a*), (dashed lines), with a theoretical transmission versus angle curve for transmitted *s* polarized light with *s* polarized incident (T_{ss}), with the director in the plane of incidence (solid line).

the discrepancies in fitting are probably not caused by measurement errors.

When fitting each mode set (ordinary or extraordinary) it is found necessary to vary the value for the liquid crystal layer thickness by 40 nm. This is not expected, since resonance and scattering into radiated light occur at a well-defined liquid crystal layer thickness, appropriate for the excitation of a Fabry–Perot mode, and so no variation in liquid crystal layer thickness should be necessary in fitting data sets. Another discrepancy is that one might expect a theoretical mode maximum to be situated at 0°—this being the mode into which the normally incident laser beam couples. This is not the case, but a change of approximately 20 nm in the liquid crystal layer thickness centres a mode about 0°, albeit displacing other higher angle modes.

Small discrepancies in fitting may be explained by the inappropriate modelling of the system. Problems arise from the fact that standard programs model an external source, with light propagating through the system in a continuous manner with respect to the input conditions. With the scattering system, the scattering centre acts as a source within the cell, and therefore phase continuity is disrupted. Also, if scattering takes place in the SiO layer, i.e. 20 nm into the cell, each order of mode is excited at a different point relative to nodes and antinodes, which is likely to perturb mode momenta, giving rise to the shifts seen. For detailed fitting, modifications to the multilayer theory are necessary, taking these factors into account.

One further piece of modelling was done, with the multilayer theory [5]. A standard one-dimensional mode modelling program was modified to generate a two-dimensional theoretical momentum space image for comparison with the data image. The 400×600 pixel image was generated by geometrically calculating azimuthal and propagation angles for each pixel. The standard program was then used to calculate the transmitted intensity for each pixel. As is clear from figure 3, the experimental data (see figure 3 (*a*)) and model theory (see figure 3 (*c*)) are very similar. This is best illustrated in figure 3 (*d*)) where we superpose a reverse contrast image; two quarters being theory and two experiment.

5. Conclusions

Momentum space imaging has been shown to be a powerful technique, capable of detecting mode details at all angles and wavelengths. Major advantages over previous angle scan techniques are a substantial time reduction for data acquisition, eradication of beam spot movement across the sample during scans, and the capture of mode details at all azimuthal angles with one cell orientation.

The technique has been used to confirm the character of a simple liquid crystal cell, and may be used in the characterization of any director profile. However some revision to theory will be necessary to model the internal scattering. The system has also revealed an enormous potential for the investigation of liquid crystal switching by fast time resolved data acquisition. Full mode information at all azimuthal angles is obtained in milliseconds, and C.C.D. line pixel scans, giving mode details at one azimuthal angle only, are achieved on the microsecond time-scale.

The authors acknowledge the financial support of the Science and Engineering Research Council in association with G.E.C. Marconi Ltd., and gratefully acknowledge the help of Dr E. L. Wood.

References

[1] WELFORD, K. R., SAMBLES, J. R., and CLARK, M. G., 1987, *Liq. Crystals*, **2**, 91.
[2] ELSTON, S. J., and SAMBLES, J. R., 1991, *Molec. Crystals liq. Crystals*, **200**, 167.
[3] ELSTON, S. J., 1991, *Liq. Crystals*, **9**, 769.
[4] LAVERS, C. R., and SAMBLES, J. R., 1990, *Liq. Crystals*, **8**, 577.
[5] KO, D. Y. K., and SAMBLES, J. R., 1988, *J. opt. Soc. Am.* A, **5**, 1863.
[6] DE GENNES, P. G., and PROST, J., 1993, *The Physics of Liquid Crystals* (Oxford Science Publications), Chap. 3.
[7] CHANDRESEKHAR, S., 1977, *Liquid Crystals* (Cambridge University Press), Chap. 3.